J|A|C|S
COMMUNICATIONS

Published on Web 05/04/2007

Ordered Mesoporous $Ce_{1-x}Zr_xO_2$ Solid Solutions with Crystalline Walls

Quan Yuan,[†] Qiang Liu,[‡] Wei-Guo Song,[‡] Wei Feng,[†] Wan-Li Pu,[†] Ling-Dong Sun,[†] Ya-Wen Zhang,[†] and Chun-Hua Yan*,[†]

Beijing National Laboratory for Molecular Sciences, State Key Laboratory of Rare Earth Materials Chemistry and Applications & PKU-HKU Joint Laboratory in Rare Earth Materials and Bioinorganic Chemistry, Peking University, Beijing 100871, China, and Institute of Chemistry, Chinese Academy of Sciences, Beijing 100080, China

Received February 8, 2007; E-mail: yan@pku.edu.cn

Great interest has been focused on the mesoporous metal oxides due to their potential application in various areas.[1] Compared to single-metal oxides, which have been widely researched,[2] multimetal oxides, such as those of the fluorite, perovskite, tetragonal, and ilmenite structures, promise the construction of robust multifunctional materials.[3] Recently, ceria-based materials are of intensive interest because they are commercially employed as the components of ultraviolet radiation absorbers, automotive three-way catalysts (TWCs), solid oxide fuel cells, and glass-polishing materials, and so forth. Particularly, ceria incorporated with zirconia are well-known to distinctly improve the thermal stability, surface area, and reducibility of the TWCs.[4] CeO_2-ZrO_2 oxides in an ordered mesoporous structure with crystalline walls are expected to provide enhanced catalytic performance due to their large surface area and a certain degree of size and shape selectivity. Sanchez et al. reported the first successful fabrication of cubic mesostructured CeO_2-ZrO_2 (rich in Zr) thin films.[5] Mesoporous $Ce_{0.5}Zr_{0.5}O_2$ with a distorted cubic structure was obtained with KLE polymer as the template.[6] Yu et al. made mesoporous $Ce_{1-x}Zr_xO_2$ with cubic structure and the corresponding $Pd/Ce_{1-x}Zr_xO_2$ catalysts for CO conversion.[7] To the best of our knowledge, no highly ordered mesoporous structures with broad ratios of cerium to zirconium have been reported so far.

In this communication, we demonstrate a novel direct and reproducible method for preparing a highly ordered mesoporous $Ce_{1-x}Zr_xO_2$ solid solution with a 2D hexagonal mesostructure. The general synthesis strategy is based on a sol−gel process combined with evaporation-induced self-assembly in ethanol using block copolymer Pluronic P123 as the template and ceric nitrate and zirconium oxide chloride as the precursors without additional acid or base. Under the optimized temperature and humidity conditions, a series of mesoporous $Ce_{1-x}Zr_xO_2$ with different Ce/Zr ratios can be obtained.

Figure 1a shows the small-angle powder X-ray diffraction (PXRD) patterns of mesoporous $Ce_{1-x}Zr_xO_2$ composites with different Ce/Zr ratios after calcined at 400 °C for 4 h. A very sharp diffraction peak appears around 1.0°, and two weak peaks are observed with $x = 0.6-0.7$, which are associated with a 2D hexagonal ($p6mm$) structure. The broadening of the (100) peak for $x = 0.4$ and 0.8 demonstrates their partly ordered mesostructure nature. These ordered mesostructures are stable up to 600 °C, while at 650 °C, the mesoporous network collapses (Figure S1 in Supporting Information).

As is well-known, the $Ce_{1-x}Zr_xO_2$ solid solutions can exist in three stable phases (monoclinic (m), tetragonal (t), cubic (c)) and two metastable phases (t', t'') under different conditions.[8] The broadening of the diffractions in wide-angle PXRD patterns (Figure 1b) indicates the nanocrystalline nature of the as-prepared samples, and thus makes it difficult to assert the crystal structure by PXRD alone. Therefore, we utilized Raman spectroscopy combined with the PXRD patterns to determine the exact phases of our $Ce_{1-x}Zr_xO_2$ samples. Six Raman-active modes ($A_{1g} + 2B_{1g} + 3E_g$) of symmetry are observed for t-ZrO_2, while for cubic CeO_2, only one F_{2g} mode centered at around 465 cm^{-1} is Raman-active.[9,10] For the sample with $x = 0.8$, the appearance of six Raman bands (Figure 1c, five located at 146, 262, 313, 459, and 630 cm^{-1} plus one shoulder at ca. 560 cm^{-1}) reveals its stable t phase nature.[11] For the samples with $x = 0.4-0.7$, the symmetric peaks in the PXRD pattern reveal their structure close to fluorite cubic phase ($c/a = 1$),[12] while their Raman bands are lying at ca. 146, 315, 455−464, and 624 cm^{-1}. The combination of Raman and XRD data demonstrates that their structure might correspond mainly to the t'' phase.[11,12] Figure 1d displays the nearly linear relationship between the cubic root of lattice volume ($V^{1/3}$) and the Zr content x of the $Ce_{1-x}Zr_xO_2$ samples, indicating the formation of $Ce_{1-x}Zr_xO_2$ ($x = 0.4-0.8$) solid solutions.

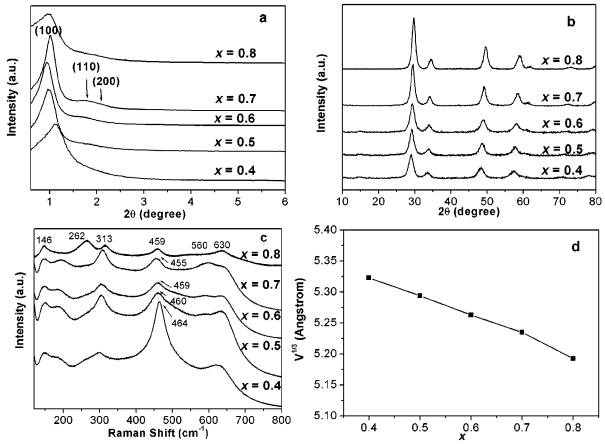

Figure 1. (a) Small- and (b) wide-angle PXRD patterns; (c) Raman spectra of mesostructured $Ce_{1-x}Zr_xO_2$ ($x = 0.4-0.8$) calcined at 400 °C; (d) cubic root of the lattice volume ($V^{1/3}$) of the $Ce_{1-x}Zr_xO_2$ ($x = 0.4-0.8$) samples calcined at 400 °C as a function of Zr content x.

Using $Ce_{0.5}Zr_{0.5}O_2$ as a representative example, the ordered mesoporous structure can be observed by TEM images. TEM images along the [001] and [110] directions (Figure 2a,b) confirm a hexagonally packed pore structure with an average diameter of about 3−4 nm over a large area, suggesting a long-range ordered mesostructure. The d_{100} values (9.0 nm) deduced from small-angle XRD (Figure 1a) can correspond well with the TEM images from the same sample (Figure 2a,b), while the slight fluctuation (7.5−9.0 nm) among samples synthesized by the same conditions indicates the high reproducibility of this synthesis method. The high-resolution TEM image (Figure S2 in Supporting Information) shows

[†] Peking University.
[‡] Chinese Academy of Sciences.

10.1021/ja070908q CCC: $37.00

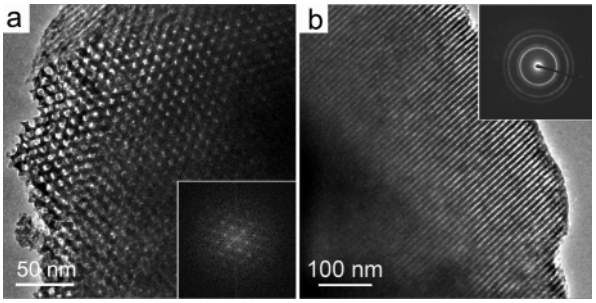

Figure 2. TEM images of the mesoporous $Ce_{1-x}Zr_xO_2$ ($x = 0.5$) recorded along the (a) [001] and (b) [110] orientations. The inset in (a) is the corresponding FFT (fast Fourier transform) diffraction image, and the one in (b) is the corresponding SAED pattern. The TEM images for the samples with other Ce/Zr ratios are shown in Figure S7.

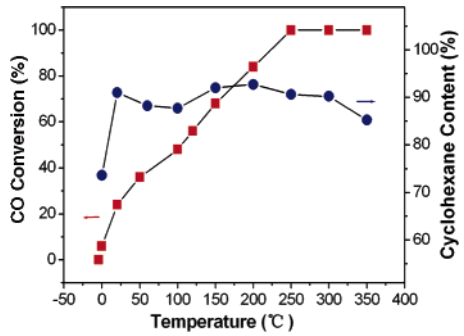

Figure 3. Catalytic activity of $Pt/Ce_{0.5}Zr_{0.5}O_2$ for CO oxidation and cyclohexene hydrogenation.

several nanocrystallites with well-defined lattice planes, demonstrating the high crystallinity of the pore walls, which is confirmed by selected area electron diffraction (SAED, the inset of Figure 2b). The nanocrystallite size is estimated to be about 3−4 nm, which is smaller than the wall thickness (ca. 6 nm, obtained from XRD and nitrogen physisorption results). Furthermore, energy dispersive X-ray (EDX) analysis (Figure S3) confirms the 1:1 molar ratio of Ce/Zr. In the mesoporous $Ce_{1-x}Zr_xO_2$ samples with different Ce/Zr ratios, large amounts of ordered mesoporous structures are also observed to coexist with some wormlike mesostructures for $x = 0.4$ and 0.8 (Figure S4).

The BET nitrogen adsorption−desorption isotherms are measured for the mesoporous $Ce_{1-x}Zr_xO_2$ ($x = 0.4$−0.8) after calcination (Figure S5). In all cases, the isotherms can be ascribed to type IV with H1-shaped hysteresis loops, implying the presence of cylindrical pores.[13] The BET surface area of the obtained crystalline mesoporous $Ce_{1-x}Zr_xO_2$ gave values of 100−130 m^2/g. Barrett−Joyner−Halenda calculations for the pore-size distribution, derived from desorption data, reveal a narrow distribution for the samples centered at 3.2−3.7 nm, which coincides well with the small-angle PXRD and TEM results of the samples.

The mesoporous $Ce_{1-x}Zr_xO_2$ solid solutions have proven to be ideal catalyst supports. Loaded with 1 wt % of 3 nm Pt nanoparticles, the Pt/*meso*-$Ce_{0.5}Zr_{0.5}O_2$ catalyst is employed for the oxidation of CO. The evolution of the CO conversion as a function of temperature is presented in Figure 3. It can be seen that at 100 °C almost 50% conversion is obtained, and 100% conversion occurs at a temperature of 250 °C. This catalyst was also tested for cyclohexene hydrogenation. The conversion rate from cyclohexene to cyclohexane increased from 74% at 0 °C to 91% at 25 °C, and then reached a plateau from 25 to 350 °C, where the byproduct of benzene (1.2−11.3%) coexists above 150 °C due to the cyclohexene dehydrogenation (Table S2). Therefore, these results strongly suggest that the ordered mesoporous $Ce_{1-x}Zr_xO_2$ supports should have potential applications in various catalytic fields.

The direct synthesis of mesoporous multi-metallic oxides or composite oxides with crystalline walls has been considered to be complicated for several reasons (such as accurate stoichiometry, highly mixable precursors, specific chemistry for each phase, and high temperature of crystallization).[3] Appropriate precursors, surfactants, and temperature enables us to obtain crystalline $Ce_{1-x}Zr_xO_2$ solid solutions with the hexagonal packed pore structure. Compared with the "acid−base pair" concept proposed in mesoporous minerals, such as the MPO system of Zhao et al.,[14] our synthesis strategy is similar to the self-adjusted process, in which there are not any extra reagents to adjust the pH of the sol−gel reaction, however, more complicated factors such as hydrolysis and coordination ability of metal ions are involved. Moreover, this simple method, through the self-adjusted formation of mesostructure, can be applied to prepare other ordered mesoporous multi-metal oxides.

Acknowledgment. This work was supported by the MOST of China (2006CB601104), NSFC (20221101, 10374006, and 2042-3005), and the Founder Foundation of PKU.

Supporting Information Available: Experimental condition; HR-TEM and EDX of $Ce_{0.5}Zr_{0.5}O_2$; TEM images of products with different Ce/Zr ratios; nitrogen adsorption−desorption isotherms combined with pore size distribution curves; TEM images of Pt/*meso*-$Ce_{0.5}Zr_{0.5}O_2$ catalyst; and products of cyclohexene hydrogenation. This material is available free of charge via the Internet at http://pubs.acs.org.

References

(1) He, X.; Antonelli, D. *Angew. Chem., Int. Ed.* **2002**, *41*, 214.
(2) (a) Huo, Q.; Margolese, D. I.; Ciesla, U.; Feng, P.; Gier, T. E.; Sieger, P.; Leon, R.; Petroff, P. M.; Schüth, F.; Stucky, G. D. *Nature* **1994**, *368*, 317. (b) Yang, P.; Zhao, D.; Margolese, D. I.; Chmelka, B. F.; Stucky, G. D. *Nature* **1998**, *396*, 152. (c) Crepaldi, E. L.; Soler-Illia, G. J. de A. A.; Grosso, D.; Cagnol, F.; Ribot, F.; Sanchez, C. *J. Am. Chem. Soc.* **2003**, *125*, 9770. (d) Sinha, A. K.; Suzuki, K. *Angew. Chem., Int. Ed.* **2005**, *44*, 271. (e) Shibata, H.; Ogura, T.; Mukai, T; Ohkubo, T.; Sakai, H.; Abe, M *J. Am. Chem. Soc.* **2005**, *127*, 16396. (f) Wang, Y.; Yang, C. M.; Schmidt, W.; Spliethoff, B.; Bill, E.; Schüth, F. *Adv. Mater.* **2005**, *17*, 53. (g) Jiao, F.; Harrison, A.; Jumas, J. C.; Chadwick, A. V.; Kockelmann, W.; Bruce, P. G. *J. Am. Chem. Soc.* **2006**, *128*, 5468. (h) Lai, X.; Li, X.; Geng, W.; Tu, J.; Li, J.; Qiu, S. *Angew. Chem., Int. Ed.* **2007**, *46*, 738.
(3) Grosso, D.; Boissière, C.; Smarsly, B.; Brezesinski, T.; Pinna, N.; Albouy, P. A.; Amenitsch, H.; Antonietti, M.; Sanchez, C. *Nat. Mater.* **2004**, *3*, 787.
(4) (a) Kašpar, J.; Fornasiero, P.; Graziani, M. *Catal. Today* **1999**, *50*, 285. (b) Kašpar, J.; Fornasiero, P.; Hickey, N. *Catal. Today* **2003**, *77*, 419.
(5) Crepaldi, E. L.; Soler-Illia, G. J. D. A.; Bouchara, A.; Grosso, D.; Durand, D.; Sanchez, C. *Angew. Chem., Int. Ed.* **2003**, *42*, 347.
(6) Brezesinski, T.; Antonietti, M.; Groenewolt, M.; Pinna, N.; Smarsly, B. *New J. Chem.* **2005**, *29*, 237.
(7) Huo, C.; Yu, J. C.; Wang, X.; Lai, S.; Qiu, Y. *J. Mater. Chem.* **2005**, *15*, 2193.
(8) (a) Yashima, M.; Morimoto, K.; Ishizawa, N.; Yoshimura, M. *J. Am. Ceram. Soc.* **1993**, *76*, 1745. (b) Yashima, M.; Morimoto, K.; Ishizawa, N.; Yoshimura, M. *J. Am. Ceram. Soc.* **1993**, *76*, 2865. (c) Yashima, M.; Arashi, H.; Kakihana, M.; Yoshimura, M. *J. Am. Ceram. Soc.* **1994**, *77*, 1067. (d) Yashima, M.; Ohtake, K.; Kakihana, M.; Yoshimura, M. *J. Am. Ceram. Soc.* **1994**, *77*, 2773.
(9) López, E. F.; Escribano, V. S.; Panizza, M.; Carnasciali, M. M.; Busca, G. *J. Mater. Chem.* **2001**, *11*, 1891.
(10) McBride, J. R.; Hass, K. C.; Poindexter, B. D.; Weber, W. H. *J. Appl. Phys.* **1994**, *76*, 2435.
(11) Martínez-Arias, A.; Fernández-García, M.; Ballesteros, V.; Salamanca, L. N.; Conesa, J. C.; Otero, C.; Soria, J. *Langmuir* **1999**, *15*, 4796.
(12) Fornasiero, P.; Balducci, G.; Di Monte, R.; Kašpar, J.; Sergo, V.; Gubitosa, G.; Ferrero, A.; Graziani, M. *J. Catal.* **1996**, *164*, 173.
(13) Sing, K. A. W.; Everett, D.; Hual, R. A. W.; Pierotti, R. A.; Rouquerol, J.; Siminiewska, T. *Pure Appl. Chem.* **1985**, *57*, 603.
(14) Tian, B.; Liu, X.; Tu, B.; Yu, C.; Fan, J.; Wang, L.; Xie, S.; Stucky, G. D.; Zhao, D. *Nat. Mater.* **2003**, *2*, 159.

JA070908Q